Journal of the Korean Society of Marine Environment & Safety
Research Paper
Vol. 27, No. 5, pp. 557-565, August 31, 2021, ISSN 1229-3431(Print) / ISSN 2287-3341(Online) https://doi.org/10.7837/kosomes.2021.27.5.557

Path-following Control for Autonomous Navigation of Marine Vessels Considering Disturbances

Sang-Do Lee*†

* Professor, Division of Navigation & Information System, Mokpo National Maritime University, Mokpo, Republic of Korea

외력을 고려한 선박의 자율운항을 위한 경로추종 제어

이상도*†

* 목포해양대학교 항해정보시스템학부 교수

Abstract : *Path-following control is considered as one of the most fundamental skills to realize autonomous navigation of marine vessels in the ocean. This study addresses with the path-following control for a ship in which there are environmental disturbances in the directions of the surge, sway, and yaw motions. The guiding principle and back-stepping method was utilized to solve the ship's tracking problem on the reference path generated by a virtual ship. For path-following control, error dynamics is one of the most important skills, and it extends to the research fields of automatic collision avoidance and automatic berthing control. The algorithms for the guiding principles and error variables have been verified by numerical simulation. As a result, most error variables converged to zero values with the controller except for the yaw angle error. One of the most interesting results is that the tracking errors of path-following control between two ships are smaller than the existing safe passing distances considering interaction forces from near passing ships. Moreover, a trade-off between tracking performance and the ship's safety should be considered for determining the proper control parameters to prevent the destructive failure of actuators such as propellers, fins, and rudders during the path-following of marine vessels.*

Key Words : *Path-following control, Autonomous navigation, Guiding principle, Error variables, Disturbances, Reference path*

요 약 : 경로추종 제어는 대양에서 선박의 자율운항을 위한 가장 기본적인 연구 중에 하나로 여겨진다. 본 연구는 선수미방향, 횡방향 및 회두방향으로 외력이 작용하는 경로추종 제어를 다룬다. 가상의 선박에서 발생하는 항로를 자선이 추종하는 문제를 해결하기 위해서 유도 원리와 백스테핑 기법을 활용하였다. 경로추종 제어에서 가장 중요한 기술 중에 하나는 오차 동역학에 관한 것으로서, 이 개념은 선박의 자동 충돌 회피 및 자동 접안 제어 등과 같은 연구 영역에서도 활용이 가능하다. 유도 원리와 오차 변수의 알고리즘은 수치 시뮬레이션을 통해 증명하였다. 그 결과, 회두각의 오차를 제외한 대부분의 오차 변수는 제어기를 통하여 제로 값으로 수렴하였다. 기존에 근거리 통항선박의 간섭력을 고려한 안전통항거리의 값보다 두 선박 간의 경로추종 제어의 트래킹 오차의 값이 더 작은 점이 가장 흥미로운 결과 중에 하나로 여겨진다. 또한 프로펠러, 핀이나 러더와 같은 엑츄에이터의 손상을 줄이기 위해서는 수렴의 성능과 선박의 안전을 절충하여 적합한 제어 파라미터를 결정할 필요가 있다.

핵심용어 : 경로추종 제어, 자율운항, 유도원리, 오차 변수, 외력, 기준 경로

1. Introduction

Very recently, a small cruiser has been successfully realized to navigate autonomously in the domestic river area (PortNews, 2021). Autonomous navigation of marine vessels is in the spotlight according to the advent of the fourth industrial revolution. Path-following control is one of the most fundamental skills to realize the autonomous navigation of marine vessels in the ocean. This study begins with the model-based approach focused on the mathematical development of path-following control rather than the possibility of application in a real ship. This paper addresses the guiding principle considering the environmental disturbances in the surge, sway, and yaw directions. The under-actuated vessel, i.e., a system with fewer actuators than degrees-of-freedom (DOF), is employed to solve the path-following problem (Aguiar and Hespanha, 2007).

† oksangdo@mmu.ac.kr, 061-240-7257

The guidance represents the basic methodology concerned with the transient behavior associated with the achievement of motion control objectives (Fossen, 2011). The guidance system of marine vessels is used to generate a predefined path for the time-invariant path following. Based on this concept, this paper shows the logical virtual ship (Zhang et al., 2015), which produces the reference path based on the way-point.

Also, it is easier to overlook the importance of error dynamics. Dynamics is concerned with bodies having accelerated motion (Fossen, 1994). During the whole path-following process, error of motions exists between the virtual ship and own ship. The guiding principle handles the error variables in closed-loop system. To converge the variables to zero, it should be defined the control system based on the error dynamics. Thus, error dynamics is the most essential concept to solve any problem of autonomous navigation such as path-following, automatic berthing, and collision avoidance.

Recently, Zheng (2020) investigated the path-following control of a surface vessel under disturbances focused on the moving reference frame, which enables applicable scenarios such as moving monitoring, aircraft carrier landing. Zhang et al. (2020) reported the way-points based path-following control of an under-actuated ship in the presence of the actuator saturation and the unknown disturbance. Zhang et al. (2015) also introduced the way-point based path-following problem of uncertain under-actuated ships in fields of marine practice. They developed the general concept of a logical virtual ship and adaptive neural networks algorithm for dynamic surface ship based on the steering law. Similarly, Li et al. (2008) studied point-to-point navigation of under-actuated ships using a general back-stepping method, containing the concise and clear physical meaning of tracking errors. Practically, the sway speed of the ship is bounded to satisfy the passive bounded condition in case that all other variables in its dynamics are bounded.

This paper ensues the methods of Zhang et al. (2015) and Li et al. (2008) to solve the problem of tracking performance and control efficiency under environmental disturbances. The reference path will be generated by a virtual (ideal) ship. The guidance concept and error dynamics algorithm have been verified by the numerical simulation.

The rest of the papers are structured as follows. In section 2, the mathematical formulation of the 3DOF system and guiding principle is briefly introduced. Section 3 presents the numerical simulations to verify the proposed path-following control scheme. Finally, some conclusions will be remarked in section 5.

2. Mathematical formulation

2.1 Dynamical ship model

The horizontal motion of a surface ship is represented by the motion components in the surge, sway, and yaw. Fig. 1 shows the motion variables in this case. Two reference frames are considered such as body-fixed frame $o_b x_b y_b z_b$ and earth-fixed frame $O_E X_E Y_E Z_E$. The origin o_b of the body-fixed frame is located at the center of gravity (CG). For marine ships, the body axes x_b, y_b and z_b are chosen to coincide with the principal axes of inertia and they are commonly defined as follows (Lee et al., 2019).

x_b - longitudinal axis (directed from aft to fore)

y_b - transverse axis (directed to starboard)

z_b - normal axis (directed to top to bottom)

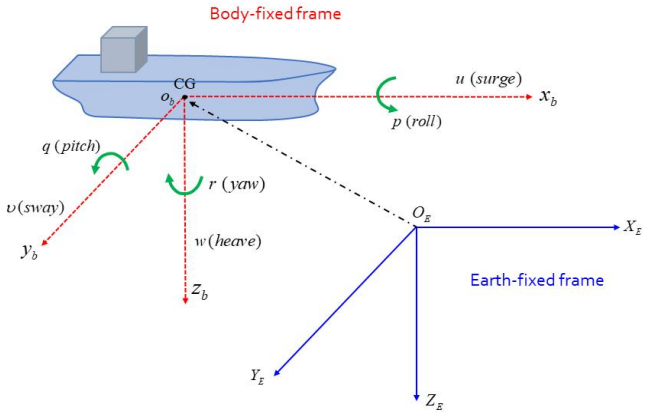

Fig. 1. Coordinate system (Fossen, 1994).

The first three coordinates (x, y, z) and their first-time derivatives correspond to the position and translational motion along x-, y- and z-axis, while the last three coordinates (ϕ, θ, ψ) and their first-time derivatives mean the orientation and rotational motion (Fossen, 2011). Since the horizontal motion of a ship can be defined as the surge, sway, and yaw motion, the state vectors are chosen as $\eta = [x, y, \psi]^T$ for the position and orientation vector and $\nu = [u, v, r]^T$ for the linear and angular velocity vector. It means that the dynamics associated with the

motion in heave (w), roll (p), and pitch (q) are ignored. The kinematic equations of motion can be reduced from the general 6DOF expression. In addition, it is assumed that the vessel has homogeneous mass distribution and xz-plane of symmetry such that $I_{xy} = I_{yz} = 0$ (Fossen, 2011). Under the assumptions, the dynamics of a surface ship moving in a horizontal plane is simplified as

$$\dot{x} = u\cos(\psi) - v\sin(\psi) \tag{1}$$

$$\dot{y} = u\sin(\psi) + v\cos(\psi) \tag{2}$$

$$\dot{\psi} = r \tag{3}$$

$$\dot{u} = f_u(\bar{\nu}) + \frac{1}{m_{11}}\tau_u + d_{w1}(t) \tag{4}$$

$$\dot{v} = f_v(\bar{\nu}) + d_{w2}(t) \tag{5}$$

$$\dot{r} = f_r(\bar{\nu}) + \frac{1}{m_{33}}\tau_r + d_{w3}(t) \tag{6}$$

with

$$f_u(\bar{\nu}) = \frac{m_{22}}{m_{11}}vr - \frac{d_{u1}}{m_{11}}u - \frac{d_{u2}}{m_{11}}u|u| - \frac{d_{u3}}{m_{11}}u^3$$

$$f_v(\bar{\nu}) = -\frac{m_{11}}{m_{22}}ur - \frac{d_{v1}}{m_{22}}v + \frac{d_{v2}}{m_{22}}v|v| - \frac{d_{v3}}{m_{22}}v^3$$

$$f_r(\bar{\nu}) = \frac{m_{11}-m_{22}}{m_{33}}uv - \frac{d_{r1}}{m_{33}}r - \frac{d_{r2}}{m_{33}}r|r| - \frac{d_{r3}}{m_{33}}r^3$$

where d_{w1}, d_{w2}, and d_{w3} denote the unknown time-varying disturbances of forces and moment; $f_u(\bar{\nu})$, $f_v(\bar{\nu})$, and $f_r(\bar{\nu})$ represent the nonlinear part including uncertainties; m_{11}, m_{22},, m_{33}, d_{u1}, d_{u2}, d_{u3}, d_{v1}, d_{v2}, d_{v3}, d_{r1}, d_{r2}, and d_{r3} mean the unknown parameters of ship's inertia, hydrodynamic damping coefficients (Zhang et al., 2015); τ_u and τ_r are actual input vector for propulsion force and yaw moment.

Remark 1. In practical, it is difficult to obtain the accurate value of time-varying environmental disturbances. In this study, the disturbances acting on the surge, sway, and yaw motion is not restricted the current itself. Ocean environmental disturbances can be considered to accommodate all aspects of navigational conditions such as waves, winds, ice-covered waters, currents and ship-to-ship interaction forces in close proximity (Lee, 2017a; Lee 2017b; Lee et al., 2020) or unexpected impact power as the transversal exciting forces (Lee et al., 2021).

Remark 2. The control input (τ_r) is considered as the total amounts of yaw moment generated by the any rudder system. Thus, specific rudder machinery model is not presented in the control scheme.

Assumption 1. $|d_{w1}| \le d_{w1\max}$, $|d_{w2}| \le d_{w2\max}$, $|d_{w3}| \le d_{w3\max}$ where $d_{w1\max}$, $d_{w2\max}$, and $d_{w3\max}$ are unknown constants (Li et al., 2008).

Assumption 2. Ship's sailing routes (reference path or trajectory) is generated by the virtual ship

$$\dot{x}_d = u_d\cos(\psi_d) \tag{7}$$

$$\dot{y}_d = u_d\sin(\psi_d) \tag{8}$$

$$\dot{\psi}_d = r_d \tag{9}$$

$$\dot{v}_d = -\frac{m_{11}}{m_{22}}u_d r_d - \frac{d_{v1}}{m_{22}}v_d + \frac{d_{v2}}{m_{22}}v_d|v_d| \tag{10}$$

where all variables are similar to the equations (1)~(6), and such that the $x_d, \dot{x}_d, \ddot{x}_d, y_d, \dot{y}_d, \ddot{y}_d$ and $\dot{\psi}_d, \ddot{\psi}_d$ exist and are all bounded (Li et al., 2008). The reference path is highly influenced by the turning rate of virtual ship (r_d).

2.2 Guiding principles and control design

Zhang et al. (2015) introduced the basic concept of straight and curve routes considering practical way-points. In Fig. 2, a virtual ship on the straight (L_{st}) goes upward with fixed forward speed (u_d) and its corresponding time ($t_s = L_{st}/u_d$). At this time, the ship's reference sailing path is generated by the virtual ship starting at a certain point (WP_i) at first. After the ship goes toward the next point (WP_{i+1}), it will move on the arc line from a curved point (P_{arc1}) and will arrive at the final point (WP_{i+2}). Then, the angle of $WP_i WP_{i+1}$ is calculated as

$$\varphi_i = \arctan\frac{y_i - y_{i-1}}{x_i - x_{i-1}} \tag{11}$$

When the virtual ship intends to alter course to starboard with turning rate (r_d), the reference path shifts from a straight line to the curve route (L_{arc}). So, the virtual ship passes through the curve points ($P_{\mathrm{arc1}}, P_{\mathrm{arc2}}$). Then, the real-time turning radius (R_{arc}) should be set to determine the turning rate (r_d) by interpolation in ($R_{\min}, R_{\max}$) as follows

$$R_{\mathrm{arc}} = \begin{cases} R_{\max} & \text{if } |\triangle\varphi_p| > \pi/2 \\ \dfrac{(R_{\max} - R_{\min})\triangle\phi_p}{sign(\triangle\phi_p)\dfrac{\pi}{2}} & \text{if } |\triangle\varphi_p| < \pi/2 \end{cases} \tag{12}$$

where $\triangle\varphi_p$ mean the practical changes of heading angle; $R_{\min}$ and $R_{\max}$ are the maximum turning radius and minimum turning radius depending on the ship's maneuvering performance (Zhang et al., 2020).

Based on the previous guidance concept, it's necessary to set the relation between virtual ship and own ship at first, as illustrated in Fig. 2. For path-following problem, error variables should be defined as

$$x_e = x_d - x\ , \qquad y_e = y_d - y\ , \tag{13}$$
$$z_e = (x_e^2 + y_e^2)^{0.5}\ , \quad \psi_e = \psi_r - \psi$$

where x_d, y_d represent the position of a virtual ship; z_e is the position error; $\psi_r (\psi_r \in (-\pi, \pi])$ mean the azimuth angle of own ship relative to the virtual ship. It is important to distinguish between the own ship's azimuth angle and yaw angle of the virtual ship (ψ_d). The own ship's azimuth angle can be obtained as

$$\psi_r = 0.5[1 - sgn(x_e)] * sgn(y_e) * \pi + \arctan(y_e / x_e) \tag{14}$$

where $sgn(\bullet)$ denotes a sign function with sgn(0)=1.

In addition, the error variables in equation (17) and $\dot{z}_e$, $\dot{\psi}_e$ can be defined as

$$x_e = z_e \cos(\psi_r), \quad y_e = z_e \sin(\psi_r) \tag{15}$$
$$\dot{z}_e = \dot{x}_d \cos(\psi_r) + \dot{y}_d \sin(\psi_r) - u\cos(\psi_e) - v\sin(\psi_e) \tag{16}$$
$$\dot{\psi}_e = \dot{\psi}_r - r \tag{17}$$

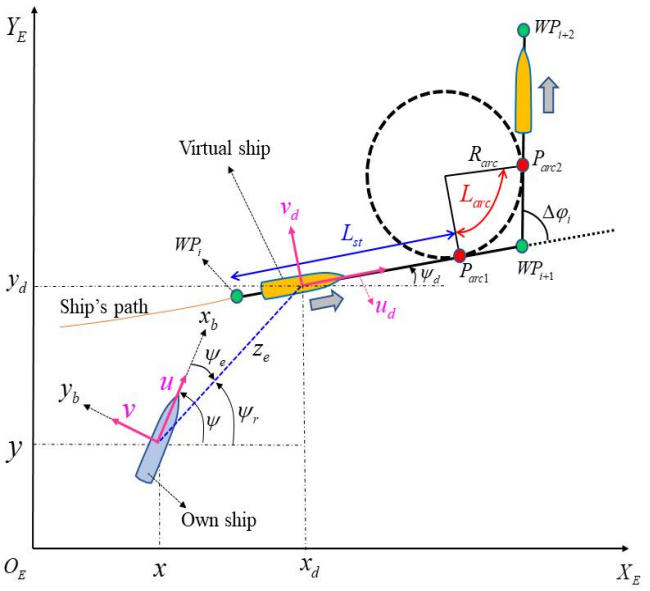

Fig. 2. Guiding concept between own ship and virtual ship.

As previously mentioned, error dynamics is one of the most valuable skills. To achieve the goal of tracking convergence, a proper control method is employed based on the concept of error dynamics. Ensued by the previous successful works of Li et al (2008) and Zhang et al (2015), a back-stepping method is considered to track the errors of surge, sway, and yaw motion. So, the virtual control inputs for surge and yaw motion should be defined as

$$\alpha_u = \frac{k_{u1}(z_e - z_m) + \dot{x}_d\cos(\psi_r) + \dot{y}_d\sin(\psi_r) - v\sin(\psi_e)}{\cos(\psi_e)} \tag{18}$$
$$\alpha_r = \dot{\psi}_r + k_{r1}\psi_e \tag{19}$$

where α_u and α_r mean the stabilizing function of surge and yaw motion, respectively; $k_{u1}, k_{r1} \geq 0$ are the design parameters; z_m is a small positive value. The control law (α_u) will stabilize the $(z_e - z_m)$ to zero. Own ship usually pursues the virtual ship by means of $(z_e - z_m)$ instead of z_e (Zhang et al., 2015). By introducing the surge and yaw velocity errors of $u_e = \alpha_u - u$ and $r_e = \alpha_r - r$, actual control inputs of own ship can be calculated as

$$\tau_u = m_{11}[k_{u2}u_e + \dot{\alpha}_u + z_e\cos\psi_e - \hat{\theta}_u f_u + \hat{d}_{w1\max}(u_e)] \tag{20}$$

$$\tau_r = m_{33}[k_{r2}r_e + \dot{\alpha}_r + \psi_e - \hat{\theta}_r f_r + \hat{d}_{w3\max}(r_e)] \quad (21)$$

with

$$\theta_u = [m_{22}/m_{11}, d_{u1}/m_{11}, d_{u2}/m_{11}]^T,$$

$$\theta_r = [(m_{11}-m_{22})/m_{33}, d_{r1}/m_{33}, d_{r2}/m_{33}]^T,$$

$$f_u = [vr, -u, -u|u|]^T \text{ and } f_r = [uv, -r, -r|r|]^T$$

where τ_u and τ_r represent the actual control inputs of surge force and yaw moment, respectively; θ_u and θ_r are unknown constant vectors with known vectors; f_u and f_r are known vectors; k_{u2} and $k_{r2} \geq 0$ are design parameters; $\hat{\theta}_u$, $\hat{\theta}_r$, $\hat{d}_{w1\max}$ and $\hat{d}_{w3\max}$ are the adaptation parts of parameters and disturbances (Li et al., 2008).

3. Simulation Tests

In this section, some simulation results will be shown to demonstrate the effectiveness of the control scheme. Table 1 represents the specification of an under-actuated ship model having one propeller and one rudder. The own ship is a patrol boat operated by the Australian customs service.

Table 1. Specifications of own ship model (patrol boat)

Parameters	Values
L_{OA} (L)	38.2 m
Beam (B, moulded)	7.2 m
Depth (D, moulded)	4.5 m
Hull draft (T, maximum)	2.3 m
Displacement ($\nabla = m/\rho$)	116.4 m^3
Speed (maximum)	24.0 knots
Range	3,000 nautical miles
Fuel consumption	0.4 tonnes/hour
Minimum turning circle (R_{arc}, radius)	150 m

3.1 Comparison of turning circles

The turning circle is a definitive maneuver that is intended to provide quantitative measures of the effectiveness of the rudder in producing steady-turning characteristics (Gertler and Gover, 1959). The rudder angle should be held constant such that a constant rate of turn is reached to a turning circle of 540° (degree) in practice (Fossen, 2011).

According to equation (12), the real-time turning radius (R_{arc}) for both patrol boat and virtual ship without disturbances is depicted in Fig. 3 (a). Unfortunately, this radius is somewhat remote from reality because the experimental data is not shown to demonstrate the simulation result. The steady turning radius would be proportional to the ship length and inversely proportional to the rudder deflection angle (Lewis, 1989). So, one of the credible results is illustrated to compare the turning circle of the Mariner class vessel (L_{OA}=171.8m, ∇=18541m^3) in Fig. 3 (b) and its maneuvering characteristics in Table 2, respectively (Fossen, 2011).

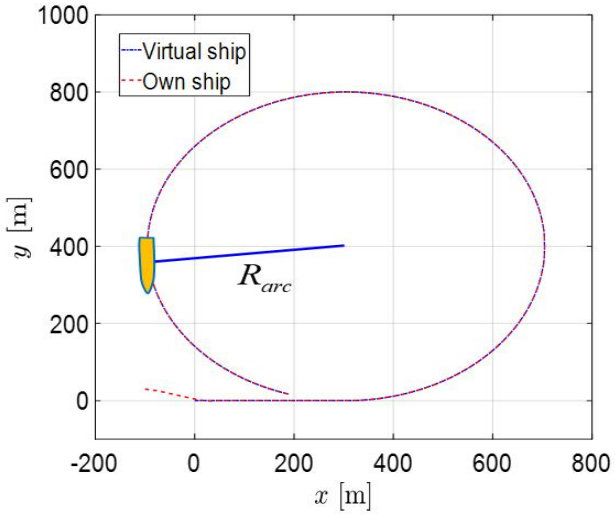

(a) Virtual ship and own ship

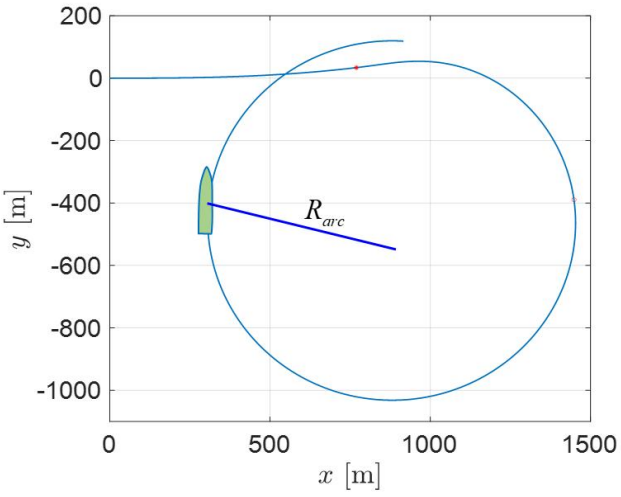

(b) Mariner class vessel

Fig. 3. Comparison of turning circles of marine vessels.

Table 2. Maneuvering characteristics of Mariner class vessel

Parameters	Values
Rudder execute	769m
Steady turning radius	711m
Maximum transfer	1315m
Maximum advance	947m
Transfer at 90 degree heading	534m
Advance at 90 degree heading	943m
Tactical diameter at 180 degree heading	1311m

3.2 Disturbances and parameter setting

The ship's sailing routes (reference path) should be set through the virtual ship, as mentioned in equations (7) to (10). The virtual ship sailing with constant forward speed ($u_d = 6\,m/s$) will generate the reference path of S-trajectory from departure way-point to arrival way-point (destination) based on the following values

$$r_d = \begin{cases} \exp\left(\dfrac{0.005t}{300}\right), & 0 \le t < 50 \;\; ; track1 \\ -0.05, & 50 \le t < 100 ; track2 \\ \left(\dfrac{0.1t}{600}\right), & 100 \le t < 266; track3 \\ 0, & 266 \le t < 400; track4 \end{cases} \tag{22}$$

This path will represent the southeast-bound straight course (track1) and show the reverse-S form trajectory (track2 and track3) until arriving at home (track4; departure way-point). The own ship starts to follow the path of the virtual ship and returns to the departure way-point within 400 seconds. Then, one can see the turning performance as well as the course-keeping ability of own ship exposed to the disturbances. During the path-following of own ship, it will be exposed to the non-zero mean time-varying disturbances in the directions of the surge, sway, and yaw motions.

$$\begin{aligned} d_{w1} &= 0.5(1 + 0.4\sin(0.2t) + 0.3\cos(0.5t)) \\ d_{w2} &= 1.5(1 + 0.3\cos(0.4t) + 0.2\sin(0.2t)) \\ d_{w3} &= -1.2(1 + 0.3\sin(0.6t) + 0.1\cos(0.5t)) \end{aligned} \tag{23}$$

Since the environmental disturbances may be different in a practical situations, the above values are selected for simple generation. Also, this control scheme is required only the boundaries of the disturbances (Do et al., 2004). Among the above disturbances, d_{w2} has the biggest effect on the course-tracking ability of own ship. The initial conditions are $[x(0), y(0), \psi(0), u(0), v(0), r(0)]$ = [-100m, 30m, -0.15rad, 0m/s, 0m/s 0rad/s]. The other parameters of initial conditions and parameters for control design are selected as in the existing literature (Li et al., 2008; Zhang et al., 2015).

$$k_{u1} = 0.2\,,\; k_{r1} = 1.8\,,\; k_{u2} = 20\,,\; k_{r2} = 120\,,$$
$$z_m = \exp(-0.054 z_e),\; d_{w1\max} = 2,\; d_{w3\max} = 3$$

3.3 Simulation results of own ship

Finally, some simulation results are depicted in Figs. 4 to 9. Fig. 4 illustrates the path-following trajectory of the actual own ship (patrol boat) in the presence of environmental disturbances in the surge, sway, and yaw directions. The patrol boat navigates east-bound in first (track1), then turns to the starboard side (track2; see zoom figure in Fig. 5) and turns to port side (track3) bound for departure way-point (track4). Even though it's difficult to come back to the exact starting way-point, it is successful to sustain that the own ship tracks the reference path in the entire sailing time.

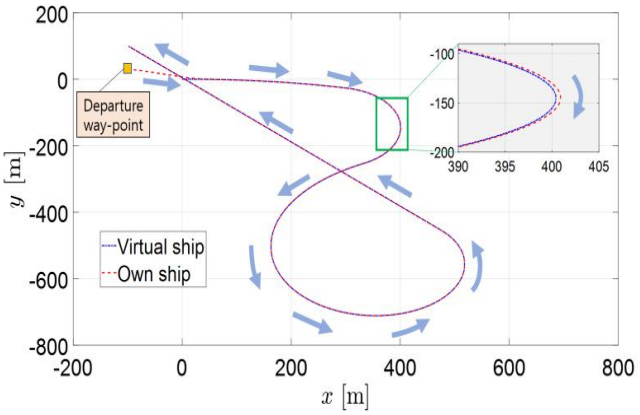

Fig. 4. Path-following trajectory of own ship (x-y coordinate).

In the path-following problem, turning cases are more difficult to reach the control goal. Thus, both track2 and track3 were arranged to show the specific control performance with the minimum and maximum values. Quantitative performance can be

seen in Table 3, where P and S mean the port and starboard side of rudder deflection, respectively. The own ship closely follows the virtual ship in turning tracks despite environmental disturbances. It is interesting to see that the tracking errors between two ships are smaller than the safe passing distances considering interaction forces from near passing ships (Lee, 2017a; 2017b).

Table 3. Performance results of own ship in turning cases

Parameters	Track2 ($50 \leq t < 100$)		Track3 ($100 \leq t < 266$)	
	Min	Max	Min	Max
x_e [m]	-0.04L	0.04L	-0.04L	0.03L
y_e [m]	-0.26B	-0.04B	-0.15B	0.15B
z_e [m]	0.03L	0.06L	0.02L	0.04L
ψ_e [degree]	-2	1	1	2.5
v_e [m/s]	-0.15	0.3	-0.3	0.15
r_e [degree/s]	0.3	0.9	0.8	0.8
τ_u [N]	-8.9E7	-7.9E6	-4.4E7	2.2E7
τ_r [Nm]	-7.1E7	4.8E8	-3.4E8	2.5E8
Rudder [degree]	1 (S)	10 (S)	8 (P)	10 (S)

Fig. 5 represents the rudder angle deflection of own ship followed by the intervals of turning rates in equation (22). However, it is not fully demonstrated because this control scheme focuses on the stabilization of error variables in the unknown parameters of the model rather than actual rudder force for yaw moment.

Figs 6 and 7 show the position and orientation errors of x_e, y_e, z_e, and ψ_e. Most error variables converge to zero values with the proposed controller except for the ψ_e. Even though the value of ψ_e does not converge to zero, it's acceptable for the patrol boat of 38.2m length overall in Fig. 7.

Then, corresponding control inputs of surge force and yaw moment are plotted in Figs. 8 and 9. The yaw control moment (τ_r) is represented to be more fluctuating than the surge control force (τ_u). Surely, when the value of k_{r1} increases, the response of τ_r will represent a more smooth curve as τ_u. However, an actuator of a patrol boat may suffer damage due to the extreme peak impact, as seen in Figs 8 and 9. Thus, a trade-off should be taken into account for selecting the proper values of control parameters. Finally, it concludes that the own patrol boat successfully tracks the reference path in the presence of environmental disturbances with the help of the proposed control scheme.

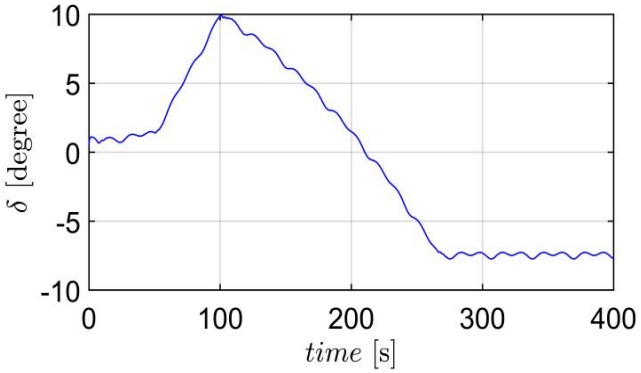

Fig. 5. Rudder angle deflection.

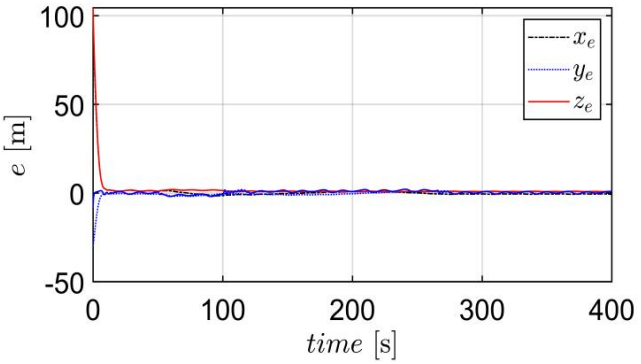

Fig. 6. Position errors of own ship.

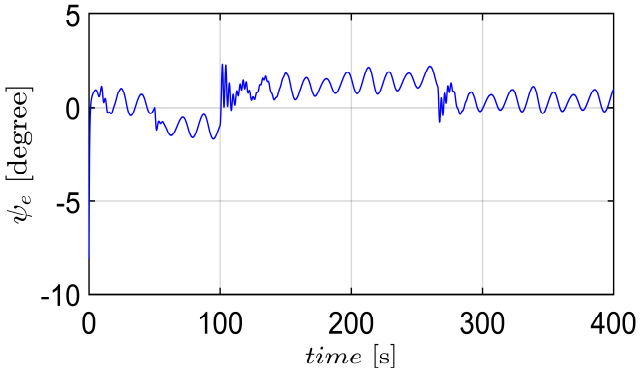

Fig. 7. Yaw angle error of own ship.

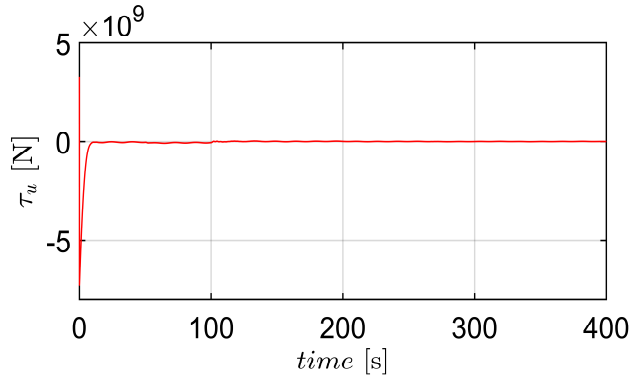

Fig. 8. Control input (τ_u , surge force) of own ship.

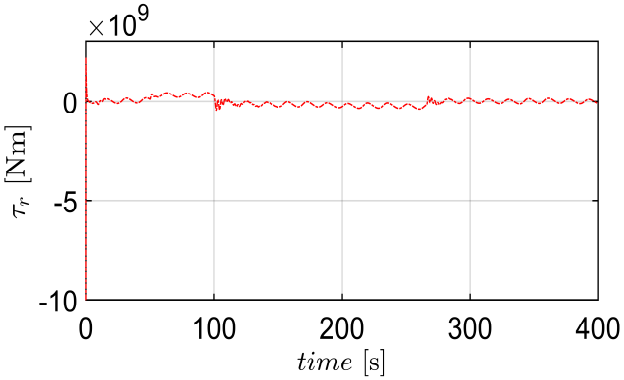

Fig. 9. Control input (τ_r , yaw moment) of own ship.

4. Conclusions

This paper investigated the path-following control of marine vessels to increase the accuracy of both course keeping and turning ability of a model ship. The scope has limited to the fundamental study focused on the mathematical development of path-following control rather than the possibility of application in a real ship. Also, rudder machinery system is not considered in this study, simulation results are not fully demonstrated in comparison with practical situation. However, the guidance algorithm in unknown parameters and unmeasurable time-varying environmental disturbances have been verified by the numerical simulations. As a result, some remarks are described as

1) The tracking errors of path-following control between two ships are smaller than the existing safe passing distances considering interaction forces from near passing ships.

2) Most error variables converge to zero with the model-based controller except for the yaw angle error. Even though the yaw angle error does not converge to zero, it is acceptable for the patrol boat of 38.2m length overall.

3) To prevent the destructive failure of actuators during the path-following, a trade-off between the tracking performance and the ship's safety should be considered for determining the appropriate control parameter values.

Finally, it concludes that the own patrol boat successfully tracks the reference path in the presence of environmental disturbances. To compensate for this study, experimental tests will be done on the real sea states shortly.

Acknowledgements

Following are results of a study on the "Leaders in INdustry-university Cooperation +" Project, supported by the Ministry of Education and National Research Foundation of Korea.

References

[1] Aguiar, A. P. and J. P. Hespanha(2007), Trajectory Tracking and Path following of underactuated Autonomous Vehicles with Parametric Modeling Uncertainty. IEEE Transactions on Automatic Control, Vol. 52, No. 8, pp. 1362-1379.

[2] Do, K. D., Z. P. Jiang, and J. Pan(2004), Robust Adaptive Path following of Underactuated Ships, Automatica, Vol. 40, pp. 929-944.

[3] Fossen, T. I.(1994), Guidance and Control of Ocean Vehicles, John Wiley & Sons Ltd, pp. 6-7.

[4] Fossen, T. I.(2011), Handbook of Marine Craft Hydro dynamics and Motion Control, First Edition, John Wiley & Sons Ltd, pp. 133-136.

[5] Gertler, M. and S. C. Gover(1959), Handling Quality Criteria for Surface Ships, Technical Report DTMB-1461, Naval Ship Research and Development Center, Washington D.C.

[6] Lee, S. D.(2017a), Simulation of Interaction Forces between Two Ships considering Ship's Dimension. Journal of Korean Society of Simulation, Vol. 26, No. 3, pp. 47-54.

[7] Lee, S. D.(2017b), A Basic Study on the Distance of Safe Passing considering Ship-to-Ship Interaction, Journal of Korean Society of Fisheries and Marine Sciences Education, Vol. 29, No. 5, pp. 1343-1355.

[8] Lee, S. D., B. D. H. Phuc, X. Xu, and S. S. You(2020), Roll Suppression of Marine Vessels using Adaptive Super-twisting Sliding Mode Control Synthesis, Ocean Engineering, Vol. 195, 106724.

[9] Lee, S. D., S. S. You, X. Xu, and T. N. Cuong(2021), Active

Control Synthesis of Nonlinear Pitch-Roll Motions for Marine Vessels, Ocean Engineering, Vol. 221, 108537.

[10] Lee, S. D., X. Xu, H. S. Kim, and S. S. You(2019), Adaptive Sliding Mode Control Synthesis of Maritime Autonomous Surface Ship, Journal of the Korean Society of Marine Environment & Safety, Vol. 25, No. 3. pp. 306-312.

[11] Lewis, E. V.(1989), Principles of Naval Architecture Second Revision, Vol. 3. Motions in Waves and Controllability, The Society of Naval Architectures and Marine Engineers, pp. 209-211.

[12] Li, J. H., P. M. Lee, B. H. Jun, and Y. K. Lim(2008), Point-to-point Navigation of Underactuated Ships, Automatica, Vol. 44. pp. 3201-3205.

[13] PortNews(2021), Steering in Information Waves, Media Group PortNews LLC, https://en.portnews.ru/news/314333/ (accessed 2021.08.11.)

[14] Zhang, G., C. Zhang, T. Yang, and W. Zhang(2020), Disturbance Observer-based Composite Neural Learning Path Following Control of Underactuated Ships subject to Input Saturation, Ocean Engineering, Vol. 216, 108033.

[15] Zhang, G., X. Zhang, and Y. Zheng(2015) Adaptive Neural Path-following Control for Underactuated Ships in Fields of Marine Practice. Ocean Engineering. Vol. 104, pp. 558-567.

[16] Zheng, Z.(2020), Moving Path Following Control for a Surface Vessel with Error Constraint, Automatica, Vol. 118, 109040.

Received : 2021. 06. 21.
Revised : 2021. 08. 19. (1st)
: 2021. 08. 24. (2nd)
Accepted : 2021. 08. 27.